The 7th World Conference on Structural Control and Monitoring, 7WCSCM,
July 22-25, 2018, Qingdao, China

Multiple Defect Size Estimation of Rolling Bearings using Autonomous Diagnosis and Vibrational Jerk

M.A.A. Ismail[a] and A. Klausen[b]

[a] Institute of Flight Systems, DLR (German Aerospace Center), 38108 Braunschweig, Germany
[b] Department of Engineering Sciences, University of Agder, 4879 Grimstad, Norway

Abstract

Developing condition monitoring techniques for monitoring ball bearings degradation is crucial to minimize unplanned down-time and maintenance costs. A recent monitoring approach is to maximize the useful service life of bearings by delaying their replacement after detecting an incipient fatigue defect, i.e. pitting/spall or wear. A variety of techniques have been investigated and reported in the literature to monitor defect size prior to a critical threshold. These studies focus on a single defect; nevertheless, the presence of multiple defects is practically experienced and its presence may introduce inaccuracies and result in wrong defect size estimation. In this paper, an autonomous fault detection technique is used to detect defect type and location, then the vibrational jerk method is extended to quantify multiple localized bearing defects. Operational spall size estimations are achieved for two defect conditions: natural run to failure defects from a test stand at University of Agder in Norway, and artificially seeded multiple spalls provided by DLR (German Aerospace Center) in Germany.

Keywords: Bearing wear, fatigue spalls, fault diagnosis, health indicator, vibration jerk

1 Introduction

Rolling element bearings are typically used in rotating machinery to transfer shaft loads to stationary housings. Bearings are therefore subject to dynamic stress that results in fatigue. In fact, up to 41% of all rotating machinery problems are related to bearing fatigue wear [1]. Operating a machine with damaged bearings increases the machine temperature, vibration, and friction losses. After further degradation, the faulted bearing may force the machine to an emergency stop due to strong vibration energy. It is therefore beneficial to monitor the condition of the bearings using condition monitoring (CM) techniques to avoid unexpected stops. The bearing vibration signal from an accelerometer is a widespread source of information for many CM techniques. Typical CM techniques involve analyzing the demodulated high-frequency resonance vibration originating from the bearing, such as the envelope spectrum [2]. CM is not only related to fault detection, but also to predict the remaining useful life after the initial fault. Spall size estimation techniques [3] can also be used to predict the degradation trend. However, multiple faults may be present in the bearing at the same time, which make it difficult to estimate the spall size from the vibration signal.

In this paper, the spall size for a bearing with multiple faults is estimated using a new technique based on monitoring the bearing unbalance. At first, the bearing vibration signal is analyzed to diagnose the bearing for faults. Afterwards, the emerging spall size is estimated for

three possible fault types. A combined trend of the spall sizes is generated, which can be used for prognostics purposes. Experimental results from two test rigs are used to verify the efficiency of the proposed method. The first test rig utilizes bearings with multiple pre-seeded faults at different spall sizes. The second test rig performs a real run to failure test, i.e. the test bearing is worn to fatigue through continuous load and operation, while vibration measurements are continually recorded.

2 Fault diagnosis algorithm

Fault diagnosis is achieved using the algorithm described in [4]. A short description of it is given here. At first, the vibration signal is order-tracked using encoder-data to transform the vibration data from the time-domain to the shaft-angle domain. The effects of speed fluctuations which smear the frequency spectrum are removed. Afterwards, the power-spectrum of the signal is obtained using the Fourier transform. Using the power-spectrum, several resonance-frequency modes are identified. For each of the resonance modes, the following steps are applied: first, the vibration signal is band-pass filtered to retain the resonance mode frequency. Subsequently, the envelope signal is calculated using the absolute-valued Hilbert transform. The envelope spectrum is further estimated by applying the Fourier transform to the envelope signal.

Faults in bearings are diagnosed by analyzing the envelope spectrum for prominent peaks at integer multiples (harmonics) of the characteristic bearing fault frequencies. With a given fault location (inner race, outer race, or roller), the envelope amplitude at integer multiples of the characteristic frequency is increased compared to the healthy state. Analyzing each envelope spectrum for increases near the characteristic frequencies is a tedious job. The algorithm in [4] describes how an autonomous process is set up to analyze each frequency-mode envelope spectrum, and calculate a score for the three different fault types. The higher the score, the more likely the given fault has occurred in the bearing. Scores below 10 are considered as noise and indicate a healthy bearing, while values over 100 suggest that a fault is present. See [4] for more detailed information.

3 Jerk-based quantification - principles

State-of-the-art studies, e.g. [5], [6], and [7], have shown that the vibration response of a spalled bearing comprises features reflecting two events that are associated with the spall width and how a ball enters and exits the spall. These events are initiated at two points: the entry point into the spall, and the exit from the spall as shown in Figure 1. Two different forms of entry/exit observations have been cited; namely, step-impulse observations and double-pulse observations [7].

In the first observation, as shown in Figure 1, the entry event induces a weak low frequency excitation, i.e. a destress. Subsequently, the ball was found to strongly strike the spall (an impact), giving rise to an impulse response, at the exit. On the other observation, the ball rolls off the leading edge and onto the exit edge of the spall with similar excitations, creating two similar pulses. The fault quantification challenge for both observations is influenced by accurately identifying the entry/exit points [5].

A recently developed approach has been developed using a Savitzky-Golay differentiator (SGD) to transform an acceleration response to a jerk response. The jerk response has better energy balanced excitations for the entry/exit events; thus making them better recognizable in comparison to raw acceleration responses. Once the fault has been detected and confirmed using well-approved methods such as envelope analysis [8], the fault size is calculated on the jerk response by the time difference between the entry and exit peaks after appropriate scaling based

on the bearing geometry, the sampling frequency and the rotational speed. A detailed investigation of jerk-based quantification has been published in [7].

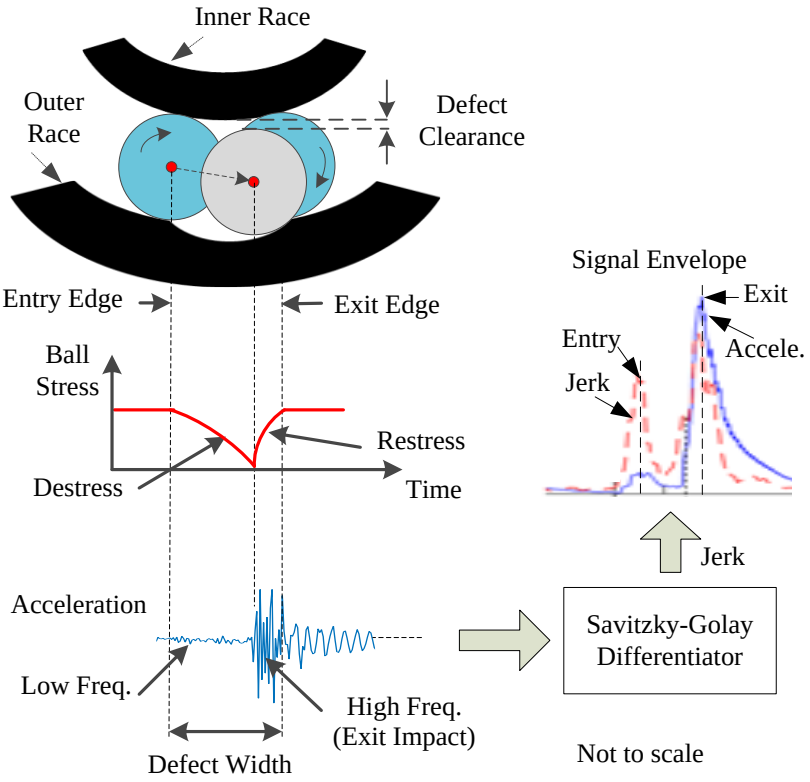

Figure 1. Vibration response of a spall defect illustrating entry/exit events and jerk-based quantification principles

4 Calibrated unbalance – a new physical degradation indicator

It was experienced that typical run to failure degradations of bearings involve multiple defects especially at advanced degradation levels [9]. Multiple defects can be multiple localized defects, e.g. pits and spalls, and may also include a distributed wear in addition to localized spalls. These defects have different vibration signatures and several health monitoring techniques have been investigated [8]. Reliable health indicators for fault prognosis demands monotonically measuring of the overall health condition.

A new concept is proposed in this paper, which monitors excessive unbalance due to bearing faults. The unbalance level can be extracted from the vibration response of the bearings in the FFT spectrum. Using the bearing unbalance as a health indicator has been investigated previously [10]; however, current methods lead to a dimensionless unbalance indicator which is influenced by the location and characteristics of the vibration sensor. Here, we propose the following steps in order to estimate a physically calibrated unbalance as a health indicator as depicted in Figure 2.

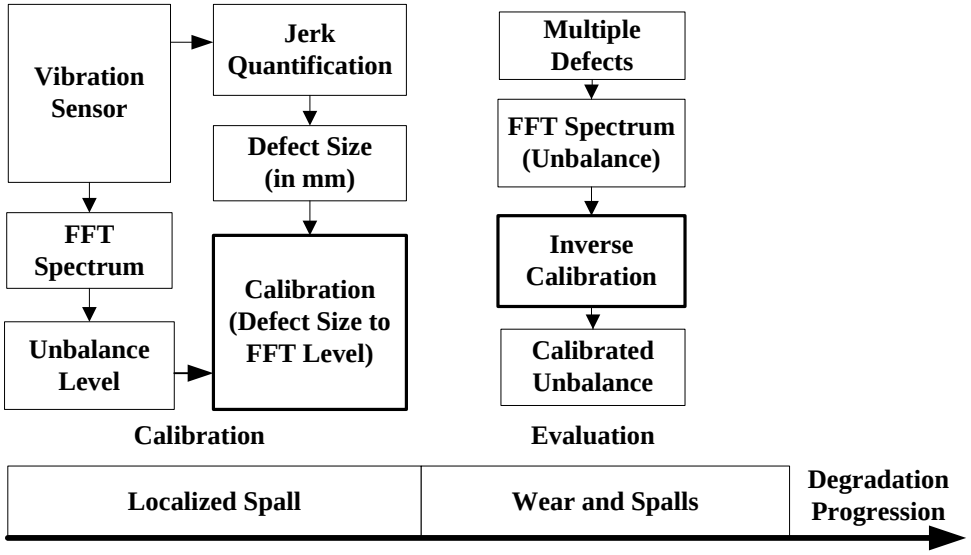

Figure 2. Proposed calibrated unbalance approach

- At an early degradation stage,
    - Localized defects are most likely to be induced. The jerk-based quantification technique is used to estimate localized defect size.
    - Localized defects create an excessive clearance and increase bearing unbalance. Defect sizes estimated by the jerk technique is fed to a bearing geometric model in order to calculate defect-related clearance.
    - The FFT spectrum of the vibration response involves a dimensionless measure, i.e. the FFT magnitude at the unbalance frequency, for defect-related clearance. The term "dimensionless measure" indicates that it is hard to physically map this value to the actual unbalance, because it depends on the unknown transmission path between the vibration sensor and the bearing elements.
    - This dimensionless measure can be calibrated by the defect-related clearances to approximate the mechanical transmission path.
- At an advanced degradation stage:
    - Multiple localized defects may be initiated in addition to a surface wear. These defects increase clearances between the bearing elements and the overall unbalance. The measured FFT magnitude for unbalance will be scaled by the aforementioned calibration to measure excessive clearances by a physical quantity.

5 Experimental Evaluations

The proposed method is evaluated using two different data types. First, seeded multi-spall defects, from DLR, that involve only an early stage as described in Figure 2. Second, a natural run to failure bearing degradation data, from University of Agder, that involve both early and advanced degradation stages.

5.1 Seeded multi-spall defects

5.1.1 Data description

Multiple seeded faults in the bearings under test (four-point FAG QJ212TVP aerospace bearings) were created by spark erosion. This formed an oval fault geometry defined by its depth and the spall width. Three different faults have been analyzed as listed in Table 1 of 500 RPM operating speed and 5 kN axial load. More details of the testing conditions and test stand can be found in [7].

Table 1. Dataset description of the multi-seeded spalls case. Additionally, the fault score for the three datasets are calculated and shown to the right in the table.

Dataset	Outer race defect [mm]		Inner race defect [mm]		Fault score		
	Width	Depth	Width	Depth	Roller	Outer race	Inner race
D0101	1.4	0.05	1.0	0.05	1.38	54442.35	52389.55
D0303	2.4	0.15	2.1	0.15	10.26	131958.76	54123.44
D0707	4.0	0.40	3.8	0.40	0.00	229388.64	11306.71

5.1.2 Fault diagnosis performance

The algorithm discussed in Section 2 is used to calculate the fault score of the three datasets in Table 1, the results are given in the right-most columns in Table 1. The results indicate that the three vibration datasets were recorded on fault-seeded bearings with an outer race fault and an inner race fault. The resulting fault diagnosis score confirms that the two defects are present in the bearing. However, the score is not monotonically increasing with larger fault size, and it is therefore necessary to quantify the fault size using the spall size estimation method.

5.1.3 Fault quantification performance

A fault quantification has been implemented for vibration datasets after confirming fault existence and its type, i.e. localized defects. Based on the jerk quantification method which is discussed in Section 3, examples of quantification results are depicted in Figure 3.

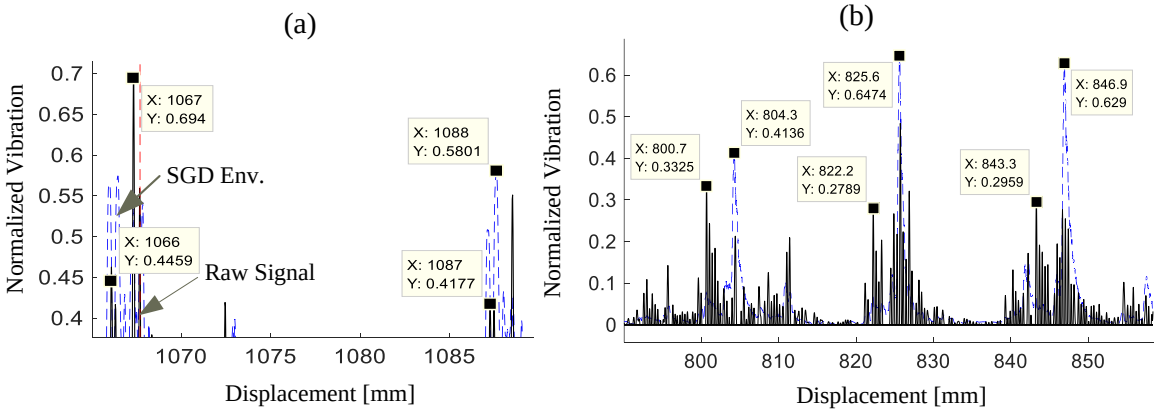

Figure 3. Examples form jerk quantification performance

Figure 3a shows two exit-spikes that are located by the raw envelope and entry-peaks that are identified by the SGD signal. The average entry-exit spacing is 1 mm which matches the average defect widths of 1.0 and 1.4 mm for the inner and outer defects respectively. Figure 3b shows three exit-spikes that are located by the aw envelope and entry-peaks that are identified

by the SGD signal. The average entry-exit spacing is 3.8 mm which matches average defect widths of 3.6 and 4.0 mm for inner and outer race defects respectively. The vibration response of D0303 includes strong background noise. The exit-spikes cannot be identified accurately in the raw vibration signal; thus the jerk method cannot be applied. The process of monitoring localized defects with the jerk method is not sufficient for monitoring multi-spall defects because indistinguishable entry/exit events.

5.2 Run to failure defects

5.2.1 Data description

The accelerated life-time data used in this paper are acquired using the test rig detailed in [11] and shown in Figure 4. The rig has been modified for this test by removing the planetary gearbox. This resulted in a less stable motor speed aiding to mimic a more realistic practical machine. A 6008 type ball bearing is naturally worn from healthy state by applying heavy radial and axial loads at a high speed of 1000 RPM. Two electric linear actuators apply a 4 kN axial load and a 9 kN radial load for the bearing. In this test, the bearing lasted roughly 41.9 million revolutions before initial damage occurred, and 42.7 million revolutions before the test was stopped due to high vibration energy. Every 30 minutes during the test, the test rig controller reduced the shaft speed to 250 rpm and measured the bearing vibration and shaft encoder pulses for the duration of 100 rounds. After the test, the bearing was disassembled to identify the faults. Pictures of the bearing are shown in Figure 5.

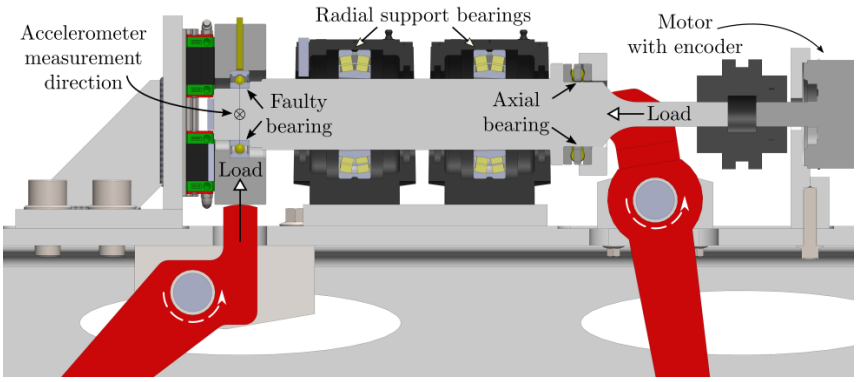

Figure 4. The bearing test rig used in the run to failure test.

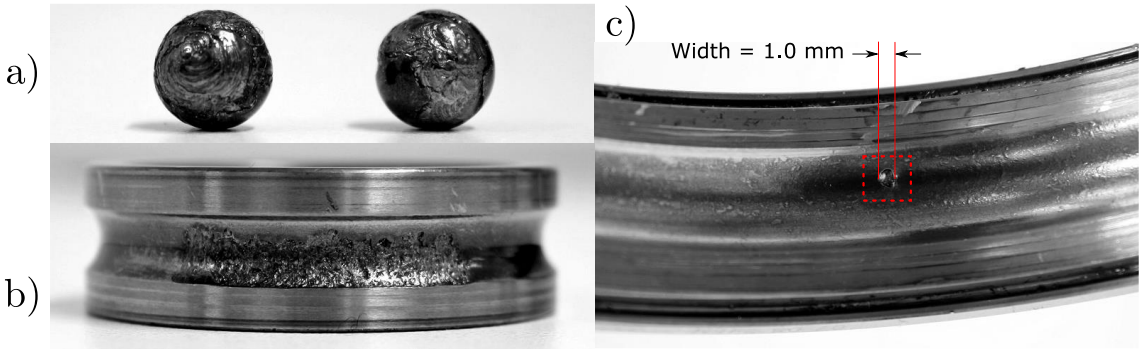

Figure 5 Faults in the de-assembled bearing after the accelerated life-time test. a) Two damaged rollers. b) Large spall area on inner race. c). Small spall on outer race with a measured width.

5.2.2 Fault diagnosis performance

The bearing fault diagnosis algorithm described in Section 2 has been used to analyze the datasets from the accelerated life-time test. The normalized fault diagnosis score is shown for the last 1.8 million revolutions in Figure 6.

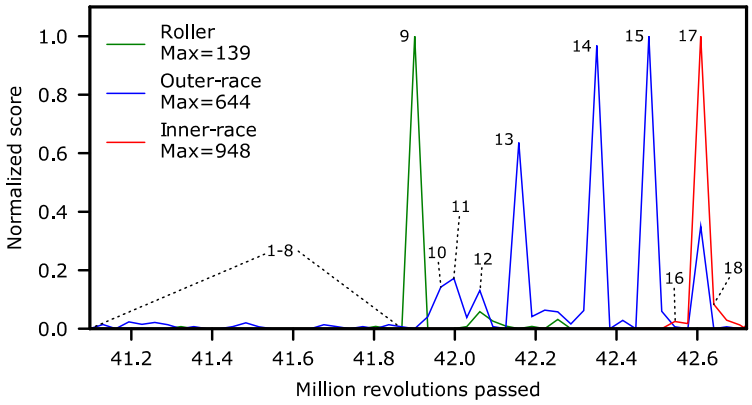

Figure 6. Normalized fault diagnosis score of the accelerated life-time dataset

The normalized fault scores (divided by maximum value as indicated in the legend) are shown for the roller fault (green), outer race fault (blue), and the inner race (red). According to this figure, a roller fault has surfaced after roughly 41.9 million revolutions as indicated by the high roller score of 139. Not long after the roller fault occurred, the outer race fault score increased. From 41.95 million revolutions to 42.5 million revolutions, the outer race fault dominates the vibration signal. Finally, an inner race fault is visible in the vibration spectrum after 42.6 million revolutions. At this stage, the bearing is very close to complete failure. The vibration recordings that are marked with numbers in Figure 6 are used for spall size estimation in the next subsection. Datasets 1 through 8 represent a healthy case, while datasets 9 through 18 represent the different damaged states.

5.2.3 Fault quantification performance

According to the diagnosis results in Figure 6, dataset #13 has been selected to evaluate the calibrated unbalance method described in Section 4. This is because the diagnosis score of dataset #13 indicated a high contribution of a localized outer race defect. Assuming that the unbalance is almost due to an outer race defect, the run to failure unbalance trend, shown in Figure 7, can be calibrated by dataset #13.

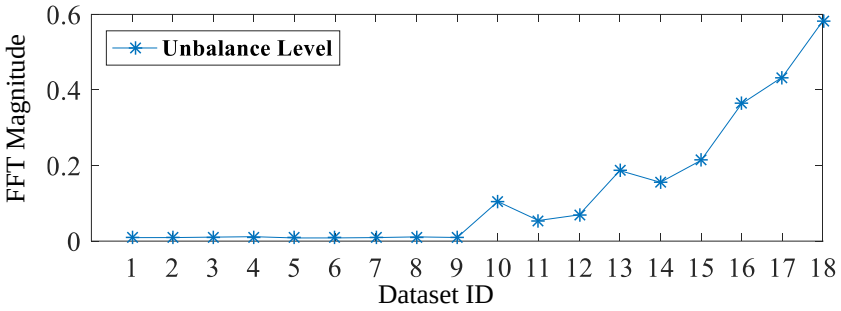

Figure 7. Run to failure unbalance levels is shown based on FFT spectrum of the vibration envelope.

The jerk performance of dataset #13 is shown in Figures 8 and 9. The average entry/exit spacing is 0.7 mm. The relation between spall-width and the radial unbalance is not linear due to different curvatures of ball diameter and bearing races. A geometric model for the bearing has been developed to map the detected spall-width (in mm) to the radial clearance (in mm). This model is shown in Figure 10. A radial clearance of 13.6 µm is present for a 0.7 mm spall width as depicted in Figure 9. The calibrated run to failure unbalance is shown in Figure 11, where nominal healthy level is less than 1 µm radial clearance, and a full failure shows at 42.45 µm clearance. This unbalance quantity does not involve the nominal clearance of ball bearing.

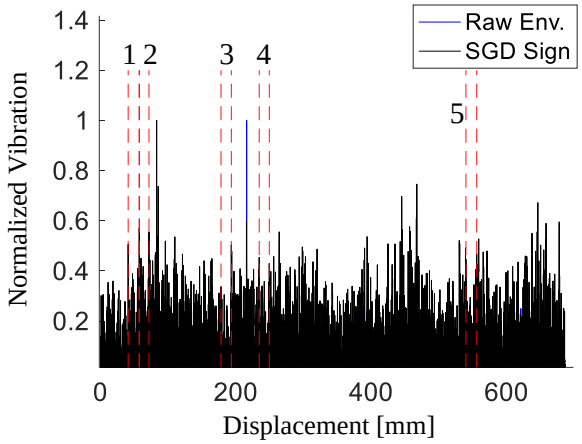

Figure 8. Vibration sample of dataset 13: a pattern recognition is used to locate most periodic outer-defect spikes (vertical dashed lines) based on zero crossing detection in the time domain.

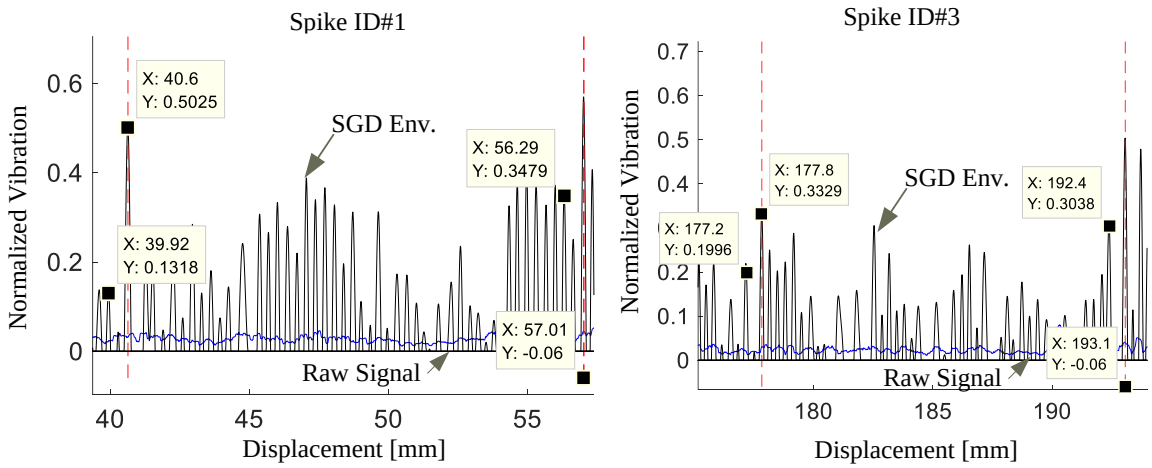

Figure 9. Vibration responses zoomed at spike ID=1, 3. Vertical dashed lines have been used as described in Figure 8 to locate spall-exit points because they are indistinguishable by raw vibration signal

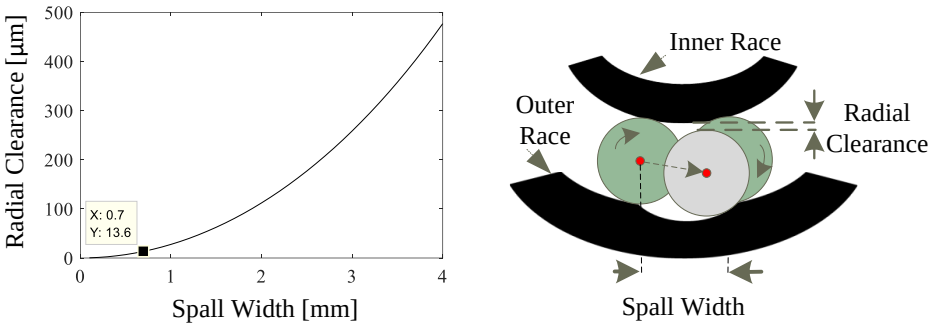

Figure 10. Simulated calculation between a spall width and the corresponding radial clearance for a bearing type 6008 assuming that the spall has a homogenous oval shape.

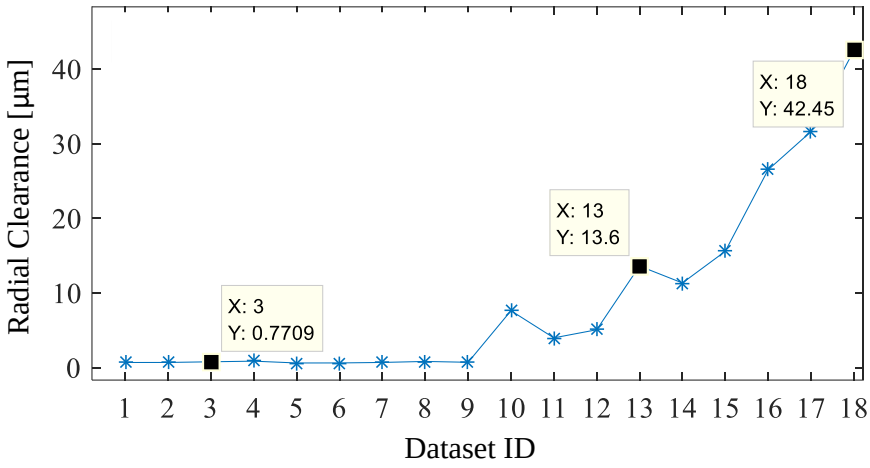

Figure 11. Run to failure unbalance after calibration

6 Conclusion

Condition monitoring of rolling element bearings is necessary to avoid sudden machine breakdown due to incipient faults. However, determining if a fault has surfaced in the bearing is not enough to quantify the severity of the fault. The spall size can be estimated using the vibrational jerk method. The referenced methods all assume that a single defect is present in the bearing. In this paper, a new method for spall size estimation of a bearing with multiple defects is presented. A radial clearance indicator is introduced, which shows how much the bearing moves from center due to multiple faults. The efficiency of the proposed method was verified using experimental datasets from two sources. The first dataset is for bearings with multiple pre-seeded faults, while the second one is a run to failure experiment where the bearing suffers from faults in all components at the end. It was shown that the radial clearance increases as the bearing wears out over time. This quantified physical indicator can be used for prognostics purposes and remaining useful lifetime estimation.

Acknowledgement

We thank the staff of TEKNIKER (IK4, Intelligent Information Systems Unit, Spain) and our colleague Ms. Thu-Hien Pham for their collaboration in preparing the database. We also

want to thank the Mechatronic Laboratory staff at the University of Agder for their help in building and preparing the test bench for the accelerated life-time test.

References

[1] R.N. Bell, D.W. McWilliams, P. O'donnell, C. Singh and S.J. Wells (1985), Report of large motor reliability survey of industrial and commercial installations. I, IEEE Transactions on Industry Applications, 21: 853–864.

[2] P.D. McFadden and J.D. Smith (1984), Model for the vibration produced by a single point defect in a rolling element bearing, Journal of Sound and Vibration, 96: 69–82.

[3] A. Chen and T.R. Kurfess (2018), A new model for rolling element bearing defect size estimation, Measurement, 114:144–149.

[4] A. Klausen, K.G. Robbersmyr and H.R. Karimi (2017), Autonomous Bearing Fault Diagnosis Method based on Envelope Spectrum, IFAC-PapersOnLine. 50:13920–13925.

[5] N. Sawalhi and R.B. Randall (2011), Vibration response of spalled rolling element bearings: Observations, simulations and signal processing techniques to track the spall size, Mechanical Systems and Signal Processing, 25:846–870.

[6] G. Kogan, J. Bortman and R. Klein (2015), Estimation of the spall size in a rolling element bearing, Insight Non-Destructive Testing and Condition Monitoring, 57:448–451.

[7] M.A.A. Ismail, A. Bierig and N. Sawalhi (2017), Automated vibration-based fault size estimation for ball bearings using Savitzky-Golay differentiators, Journal of Vibration and Control, doi: 10.1177/1077546317723227.

[8] R.B. Randall and J. Antoni (2011), Rolling element bearing diagnostics - A tutorial, Mechanical Systems and Signal Processing, 25:485–520.

[9] C. Hatch, A. Weiss and M. Kalb (2010), Cracked bearing race detection in wind turbine gearboxes, Orbit. 30:40-47.

[10] S.P. Mogal and D.I. Lalwani (2015), Experimental investigation of unbalance and misalignment in rotor bearing system using order analysis, Journal of Measurement Engineering, 3:114–122.

[11] A. Klausen, R.W. Folgerø, K.G. Robbersmyr and H.R. Karimi (2017), Accelerated Bearing Life-time Test Rig Development for Low Speed Data Acquisition, Modeling, Identification and Control, 38:143–156.